

The Impact of HI in Galaxies on 21-cm Intensity Fluctuations During the Reionisation Epoch

J.S.B. Wyithe^{1*}, L. Warszawski¹, P.M. Geil¹, S. Peng Oh²

¹*School of Physics, University of Melbourne, Parkville, VIC 3010, Australia*

²*Department of Physics, University of California, Santa Barbara, CA 93106, USA.*

6 November 2018

ABSTRACT

We investigate the impact of neutral hydrogen (HI) in galaxies on the statistics of 21-cm fluctuations using analytic and semi-numerical modelling. Following the reionisation of hydrogen the HI content of the Universe is dominated by damped absorption systems (DLAs), with a cosmic density in HI that is observed to be constant at a level equal to $\sim 2\%$ of the cosmic baryon density from $z \sim 1$ to $z \sim 5$. We show that extrapolation of this constant fraction into the reionisation epoch results in a reduction of 10-20% in the amplitude of 21-cm fluctuations over a range of spatial scales. The assumption of a different percentage during the reionisation era results in a proportional change in the 21-cm fluctuation amplitude. We find that consideration of HI in galaxies/DLAs reduces the prominence of the HII region induced *shoulder* in the 21-cm power spectrum (PS), and hence modifies the scale dependence of 21-cm fluctuations. We also estimate the 21cm-galaxy cross PS, and show that the cross PS changes sign on scales corresponding to the HII regions. From consideration of the sensitivity for forthcoming low-frequency arrays we find that the effects of HI in galaxies/DLAs on the statistics of 21-cm fluctuations will be significant with respect to the precision of a PS or cross PS measurement. In addition, since overdense regions are reionised first we demonstrate that the cross-correlation between galaxies and 21-cm emission changes sign at the end of the reionisation era, providing an alternative avenue to pinpoint the end of reionisation. The sum of our analysis indicates that the HI content of the galaxies that reionise the universe will need to be considered in detailed modelling of the 21-cm intensity PS in order to correctly interpret measurements from forthcoming low-frequency arrays.

Key words: cosmology: diffuse radiation, large scale structure, theory – galaxies: High redshift, inter-galactic medium

1 INTRODUCTION

The process of hydrogen reionisation is thought to have started with ionised (HII) regions around the first galaxies, which later grew to surround groups of galaxies. Reionisation completed once these HII regions overlapped and occupied most of the volume between galaxies. Much recent theoretical attention has focused on the power spectrum (PS) of 21-cm emission from neutral hydrogen (HI) during the reionisation era (Zaldarriaga, Furlanetto & Hernquist 2004; Furlanetto et al. 2004; Morales et al. 2005; Bowman et al. 2006). In particular, the ionisation structure of the intergalactic medium (IGM) owing to UV emission as-

sociated with star formation has been studied in detail using analytic (Furlanetto et al. 2004; Barkana 2007), numerical (McQuinn et al. 2006; Iliev et al. 2008), and more recently, semi-numerical models (Zahn et al. 2007; Mesinger & Furlanetto 2007; Geil & Wyithe 2008).

These studies describe a scenario in which very large HII regions form around clustered sources within overdense regions of the IGM. The formation of these HII regions has a significant effect on the shape of the 21-cm PS because information on the small scale features in the density field is erased from the signal originating within the ionised regions. Conversely, the creation of large ionised regions imprints large scale features on the distribution of 21-cm intensity. The sum of these effects is to move power from small to large scales, leaving a shoulder shaped feature on the PS

* swyithe@unimelb.edu.au

at the characteristic scale of the H II regions (Furlanetto et al. 2004). The detailed morphology of the ionisation structure will therefore yield information about both the ionising sources and the structure of absorbers in the IGM on small scales (McQuinn et al. 2006). As reionisation leaves a strong imprint on the 21-cm PS, measuring the latter has become a key goal for learning about the reionisation epoch (Furlanetto, Oh & Briggs 2006, and references therein). In addition, since reionisation is driven by galaxy formation, whose statistics reflect those of the underlying density field, the detection of the redshifted 21-cm signal will not only probe the astrophysics of reionisation, but also the matter PS during the epoch of reionisation (McQuinn et al. 2006; Bowman, Morales & Hewitt 2007). Finally, it has been recognised that cross-correlating galaxy surveys with 21-cm maps could yield powerful new insights into the morphology of reionisation, as well as eliminate some of the difficulties related to foreground removal (Furlanetto & Lidz 2007; Wyithe & Loeb 2007; Lidz et al 2008). With these ideas as motivation, several experiments are currently under development that aim to detect the 21-cm signal during reionisation, including the Low Frequency Array¹ (LOFAR), the Murchison Widefield Array² (MWA) and the Precision Array to Probe Epoch of Reionization³ (PAPER), and more ambitious designs are being planned such as the Square Kilometer Array⁴ (SKA).

Up until now only the component of H I residing in the IGM has been considered in relation to forecasts of the statistical 21-cm signal. However, after the completion of reionisation there is known to be a residual H I fraction of a few percent in high density clumps which are believed to reside within galaxies (e.g., Prochaska et al 2005). This high density contribution to the H I content of the Universe is also present during the reionisation era (we refer to this high density H I as *galactic H I* throughout the paper). Moreover, because galaxies at high redshift are biased relative to the density field, this galactic H I contribution could provide a significant perturbation to the predicted statistics of 21-cm fluctuations.

Wyithe & Loeb (2007) have modelled the density dependent reionisation process using a semi-analytic model that incorporates the important physical processes associated with galaxy bias and radiative feedback. In agreement with numerical simulations (McQuinn et al. 2006; Iliev et al. 2008), this model demonstrates that galaxy bias leads to enhanced reionisation in overdense regions. In this paper we use this model and its semi-numerical extension to explore the effect that the H I content of the biased galactic sources of reionisation would have on the fluctuations in redshifted 21-cm emission. We begin by describing our density dependent model of reionisation in § 2. We then summarise the observed evolution of the H I density in § 3, and our results for the evolution of the 21-cm signal in § 4. We next describe the effect of galactic H I on the 21-cm signal using analytic and semi-numerical models in § 5-7, and discuss prospects for detection in § 8. We conclude in § 9. Throughout this paper

we adopt a concordance cosmology for a flat Λ CDM universe, $(\Omega_m, \Omega_\Lambda, \Omega_b, h, \sigma_8, n) = (0.27, 0.73, 0.046, 0.7, 0.8, 1)$, consistent with the constraints from Komatsu et al. (2008). All distances are in comoving units unless stated otherwise.

2 DENSITY DEPENDENT ANALYTIC MODEL OF REIONISATION

In regions of the IGM that are overdense, galaxies will be over-abundant for two reasons: first because there is more material per unit volume to make galaxies, and second because small scale fluctuations need to be of lower amplitude to form a galaxy when embedded in a larger scale overdensity (the so-called *galaxy bias*; see Mo & White 1996). Regarding reionisation of the IGM, the first effect will result in a larger density of ionising sources. However this larger density will be compensated by the increased density of gas to be ionised, which also increases the recombination rate. The process of reionisation also contains several layers of feedback. Radiative feedback heats the IGM and results in the suppression of low-mass galaxy formation (Efstathiou, 1992; Thoul & Weinberg 1996; Quinn et al. 1996; Dijkstra et al. 2004). Such feedback effects can potentially be more intense in overdense regions, leading to weaker galaxy formation bias than might be expected from simple linear bias models (Kramer et al 2006). Probing the morphology of reionisation could potentially lead to constraints on such feedback effects.

To compute the relation between the local overdensity and the brightness temperature of redshifted 21-cm emission we use the model described in Wyithe & Loeb (2007). Here we summarise the main features of the model, and describe the additions made for the purpose of including the possible contribution from galaxies. The evolution of the ionisation fraction by mass $Q_{\delta,R}$ of a particular region of IGM with scale R and overdensity δ (at observed redshift z_{obs}) may be written as

$$\begin{aligned} \frac{dQ_{\delta,R}}{dt} &= \frac{N_{\text{ion}}}{0.76} \left[Q_{\delta,R} \frac{dF_{\text{col}}(\delta, R, z, M_{\text{ion}})}{dt} \right. \\ &\quad \left. + (1 - Q_{\delta,R}) \frac{dF_{\text{col}}(\delta, R, z, M_{\text{min}})}{dt} \right] \\ &\quad - \alpha_B C n_{\text{H}}^0 \left(1 + \delta \frac{D(z)}{D(z_{\text{obs}})} \right) (1+z)^3 Q_{\delta,R}, \end{aligned} \quad (1)$$

where N_{ion} is the number of photons entering the IGM per baryon in galaxies, α_B is the case-B recombination coefficient, $C = 2$ is the clumping factor (which we assume, for simplicity, to be constant), and $D(z)$ is the growth factor between redshift z and the present time. The production rate of ionising photons in neutral regions is assumed to be proportional to the collapsed fraction F_{col} of mass in halos above the minimum thresholds in neutral (M_{min}), and in ionised (M_{ion}) regions. We assume M_{min} to correspond to a virial temperature of 10^4 K, representing the hydrogen cooling threshold, and M_{ion} to correspond to a virial temperature of 10^5 K, representing the mass below which infall is suppressed from an ionised IGM (Dijkstra et al. 2004). In a region of co-moving radius R and mean overdensity $\delta(z) = \delta D(z)/D(z_{\text{obs}})$ [specified at redshift z instead of the usual $z = 0$], the relevant collapsed fraction is obtained

¹ <http://www.lofar.org/>

² <http://www.haystack.mit.edu/ast/arrays/mwa/>

³ <http://astro.berkeley.edu/~dbacker/eor/>

⁴ <http://www.skatelescope.org/>

from the extended Press-Schechter (1974) model (Bond et al. 1991) as

$$F_{\text{col}}(\delta, R, z) = \text{erfc} \left(\frac{\delta_c - \delta(z)}{\sqrt{2([\sigma_{\text{gal}}]^2 - [\sigma(R)]^2)}} \right), \quad (2)$$

where $\text{erfc}(x)$ is the complementary error function, $\sigma^2(R)$ is the variance of the density field smoothed on a scale R , and σ_{gal}^2 is the variance of the density field smoothed on a scale R_{gal} , corresponding to a mass scale of M_{min} or M_{ion} (both evaluated at redshift z rather than at $z = 0$). In this expression, the critical linear overdensity for the collapse of a spherical top-hat density perturbation is $\delta_c \approx 1.69$.

The model assumes that on large (linear regime) scales most ionising photons are absorbed locally, so that the ionisation of a region is caused by nearby ionisation sources. This assumption is certainly justified during the early stages of reionisation, when the mean free path for ionising photons is short. However, even later in the reionisation process, the mean free path always remains smaller than the characteristic H II bubble size (it could be smaller if mini-halos or pockets of residual H I block ionising photons between the sources and the edge of the H II region.) Our local ionisation assumption is therefore valid as long as the characteristic bubble size is smaller than the spatial scale of the correlations we consider. This requirement is met in regimes where the fraction of regions at a particular scale are fully ionised is very low. This point is discussed quantitatively in Wyithe & Morales (2007).

3 THE H I CONTENT OF GALAXIES

Following the completion of reionisation, around 2% of the hydrogen content of the Universe is observed to be in H I within galaxies. Moreover, this two percent fraction is observed to be roughly constant from $z \sim 1$ to $z \sim 5$ (e.g. Prochaska et al. 2005). However, to estimate the effect of galactic H I on 21-cm fluctuation statistics during the reionisation epoch we must extrapolate to higher redshift. There are two competing factors. On the one hand the collapsed fraction of mass rises as reionisation progresses, which would imply a galactic H I fraction that decreases towards high redshift. On the other hand, the fact that the H I fraction is constant below $z \sim 5$ suggests that the fraction of hydrogen within galaxies that is in H I increases with redshift. In this paper we conservatively assume that the fraction of gas within galaxies that is H I increases at a rate that preserves the 2% galactic H I mass fraction (relative to the total hydrogen content of the Universe) into the reionisation epoch. At redshifts where there is not a sufficient collapsed fraction to maintain the 2% value, the galactic H I fraction is allowed to drop below 2%.

This is obviously a fairly simplistic model. The actual physics of the H I content in galaxies depends both on star formation and feedback processes within the galaxy, as well as on the intergalactic UV background. For instance, as the UV background falls toward high redshift, the H I fraction within galaxies could increase, and perhaps conspires to cancel with the decreasing collapse fraction to maintain the observed roughly constant H I fraction of $\sim 2\%$, as seen from $z \sim 1 - 5$. Indeed, the fraction in protogalactic H I may be

even larger than the $\sim 2\%$ we assume in the pre-reionisation epoch, particularly if there is a significant population of minihalos⁵ with $T_{\text{vir}} < 10^4 \text{K}$. Modelling this quantity is difficult and beyond the scope of this paper. For now, we note that our empirical extrapolation becomes increasingly uncertain at high redshift; it is probably reasonable in the redshift range $z \sim 6 - 8$, where some of the most interesting effects (such as the change of sign of the cross-correlation between galaxies and 21-cm emission) take place.

4 EVOLUTION OF THE 21-CM INTENSITY SIGNAL

To illustrate the contribution of galactic H I, we use the following example. We first find the value of N_{ion} that yields overlap of ionised regions at the mean density IGM by $z \sim 6$ (Fan et al. 2006; Gnedin & Fan 2006; White et al. 2003), and then integrate equation (1) as a function of δ and R . At a specified redshift, this yields the filling fraction of ionised regions within the IGM on various scales R as a function of overdensity. We may then calculate the corresponding 21-cm brightness temperature contrast owing to H I in both the IGM and galaxies

$$T(\delta, R) = 22\text{mK} \left(\frac{1+z}{7.5} \right)^{1/2} \times \left(1 - Q_{\delta, R} - Q_{\delta, R}^{\text{col}} \right) \left(1 + \frac{4}{3}\delta \right), \quad (3)$$

where the pre-factor of $4/3$ on the overdensity refers to the spherically averaged enhancement of the brightness temperature due to peculiar velocities in overdense regions (Bharadwaj & Ali 2005; Barkana & Loeb 2005), and $1 - Q_{\delta, R}^{\text{col}}$ is the mass averaged fraction of H I in galaxies relative to the total hydrogen content of the Universe. Note that we only account for brightness temperature fluctuations due to variation in the density and ionisation fraction of the IGM. We ignore variations in the spin temperature (which we assume to be always much greater than the CMB temperature) due to fluctuations in heating and radiative Ly α coupling; these are important primarily early in the reionisation process, when galaxies are in any case rare.

4.1 The auto-correlation function of 21-cm intensity fluctuations

Since the underlying probability distribution of overdensities $dP/d\delta$ is known (a Gaussian of variance σD), we may compute the observed probability distribution for T ,

$$\frac{dP}{dT}(\theta) \propto \frac{dP}{d\delta} \left| \frac{\partial \delta}{\partial T} \right|. \quad (4)$$

The second moment of this distribution corresponds to the auto-correlation function of brightness temperature

⁵ Since these are photoevaporated as reionisation progresses (Shapiro et al 2004), they will reside primarily in neutral regions, and present an additional biased H I contribution that is anti-correlated with galaxies but which we do not model here.

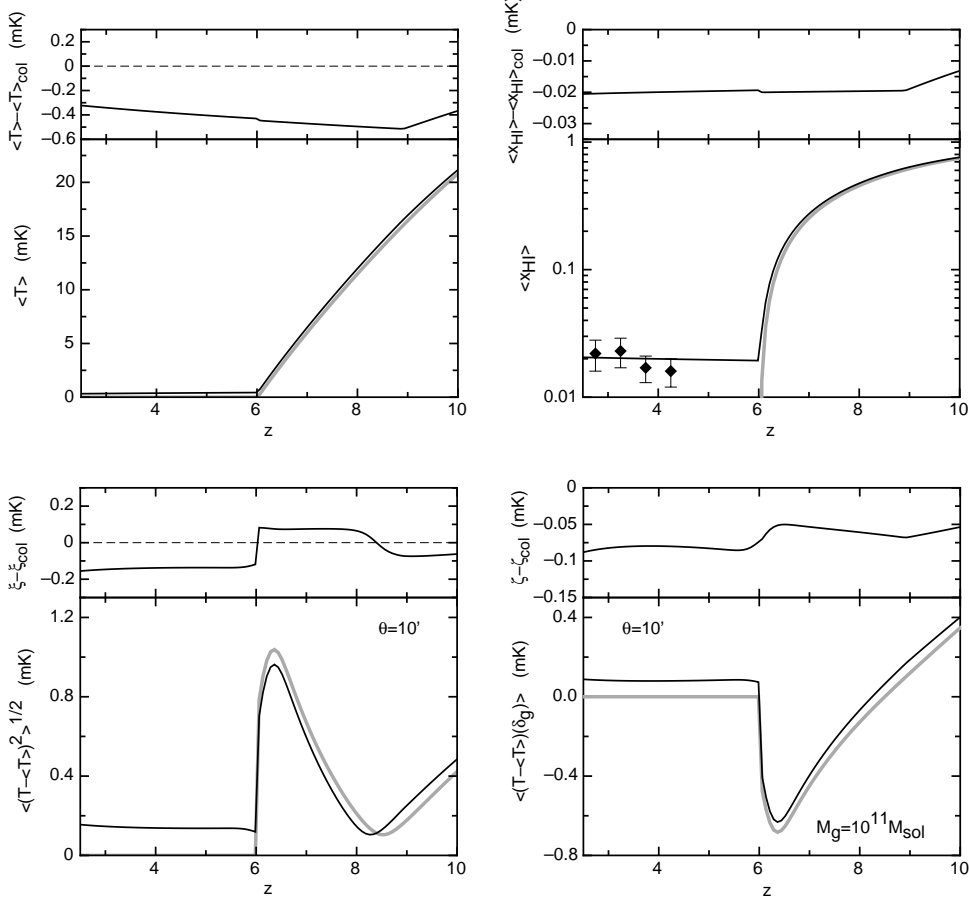


Figure 1. Model-I associating galactic HI with star forming galaxies. *Upper Left:* The evolution of the mean brightness temperature with redshift. *Upper Right:* The evolution of the mean HI fraction with redshift. The observed points are inferred from observations of damped Ly α absorbers (Prochaska et al. 2005). *Lower Left:* The evolution of the auto-correlation function of brightness temperature with redshift (computed within regions of size $10'$). *Lower Right:* The evolution of the cross-correlation function with redshift (computed within regions of size $10'$). In each case the grey and dark lines correspond to models which exclude and include the galactic HI respectively. The small upper sections of each panel show the difference between the models without galactic HI and including galactic HI.

smoothed on an angular radius θ :

$$\xi \equiv \langle (T - \langle T \rangle)^2 \rangle = \left[\frac{1}{\sqrt{2\pi}\sigma(R)} \int d\delta (T(\delta, R) - \langle T \rangle)^2 e^{-\frac{\delta^2}{2\sigma(R)^2}} \right], \quad (5)$$

where

$$\langle T \rangle = \frac{1}{\sqrt{2\pi}\sigma(R)} \int d\delta T(\delta, R) e^{-\frac{\delta^2}{2\sigma(R)^2}}, \quad (6)$$

and $\sigma(R)$ is the variance of the density field (at redshift z) smoothed on a scale R .

4.2 The cross-correlation between galaxies and 21-cm intensity fluctuations

The inclusion of galactic HI in the calculation of the 21-cm signal will also modify predictions for the cross-correlation of 21-cm emission with galaxies. The cross-correlation function of galaxy overdensity and brightness temperature smoothed

on an angular radius θ is

$$\zeta \equiv \langle (T - \langle T \rangle) \delta_g \rangle = \left[\frac{1}{\sqrt{2\pi}\sigma(R)} \int d\delta (T(\delta, R) - \langle T \rangle) \times \frac{4}{3} \delta_g e^{-\frac{\delta^2}{2\sigma(R)^2}} \right], \quad (7)$$

where $\delta_g = b\delta$, and $b(M_g, z)$ is the galaxy bias for a halo of mass M_g at redshift z (Sheth, Mo & Tormen 2001). To calculate the cross-correlation function we assume $M_g = 10^{11} M_\odot$ for the host mass of observed galaxies throughout this paper. This host mass yields a density of galaxies that is comparable to the density observed in the Subaru Deep Fields (Kashikawa et al. 2006) at $z \sim 6.6$ (Furlanetto & Lidz 2007).

5 MODEL-I: GALACTIC HI ASSOCIATED WITH STAR FORMING GALAXIES

In this section we use our analytic model to estimate the effect of galactic HI on 21-cm fluctuations. We assume that the star forming galaxies responsible for reionisation are the harbourers of galactic HI, and calculate the fraction of galac-

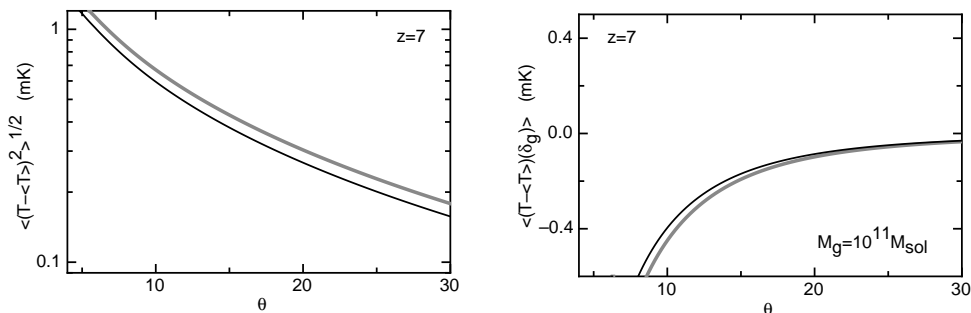


Figure 2. Model-I associating galactic HI with star forming galaxies. *Left:* The angular dependence of the auto-correlation function of brightness temperature (computed at $z = 7$). *Right:* The angular dependence of the cross-correlation function (computed at $z = 7$). In each case the grey and dark lines correspond to models which exclude and include the galactic HI respectively.

tic hydrogen that is in HI form

$$f_{\text{HI,col}} = \min \left(1, \frac{0.02}{F_{\text{col}}(z, M_{\text{min}})(1-Q) + F_{\text{col}}(z, M_{\text{ion}})Q} \right), \quad (8)$$

where F_{col} and Q are computed for the mean universe ($\delta = 0$, $R = \infty$). This enforces the condition that the fraction of HI in galaxies is either $\sim 2\%$, or equal to the (lower) collapse fraction in galaxies. We can then compute the fraction of cosmic hydrogen that is galactic HI in regions of overdensity δ and radius R

$$1 - Q_{\delta,R}^{\text{col}} = f_{\text{HI,col}} [Q_{\delta,R} F_{\text{col}}(\delta, R, z, M_{\text{ion}}) + (1 - Q_{\delta,R}) F_{\text{col}}(\delta, R, z, M_{\text{min}})]. \quad (9)$$

This contribution to the HI fraction of the Universe can be used with equation (14) to estimate the effect of galactic HI on the statistics of 21-cm emission.

The evolution of mean brightness temperature, together with the mean HI fraction $\langle x_{\text{HI}} \rangle = 1 - Q - Q^{\text{col}}$ are plotted in Figure 1. The data points show the observed fraction from damped Ly α absorbers for comparison (Prochaska et al 2005). The solid dark lines show the case including the galactic HI contribution. The thick grey line shows the IGM-only model for comparison. The residuals plotted above each panel show the magnitude of the effect when the galaxy contribution is ignored. The inclusion of galactic HI increases the global 21-cm signal slightly as expected.

Examples of auto-correlation functions are shown in Figures 1 and 2. The auto-correlation function is plotted as a function of redshift at $\theta = 10'$ (Figure 1), and as a function of θ at $z = 7$ (Figure 2). In Figure 1 the residuals are plotted above each panel to show the magnitude of the error introduced when the galaxy contribution is ignored. Early in the reionisation process, before the appearance of H II regions begins to dominate the fluctuation amplitude, the inclusion of a galactic fraction enhances the 21-cm fluctuations. However, in contrast to the mean signal, the size of fluctuations are reduced by the presence of galaxies late in the reionisation era. This reduction can be traced to the fact that galaxies are biased towards overdense regions, while neutral IGM is biased towards underdense regions which are reionised last. As a result, the inclusion of a galactic HI fraction reduces the intensity contrast between overdense and underdense regions. The size of the residuals shows that

within this model, the 2% galactic HI fraction reduces the fluctuation amplitude over a large fraction of the reionisation epoch. At $z \sim 7$, it reduces the fluctuation amplitude by around 10% at all angles (which makes sense, since galactic HI constitutes about $\sim 10\%$ of the total HI content of the universe at that point).

Examples of the cross-correlation functions are shown in Figure 1 as a function of redshift at fixed angle ($\theta = 10'$), and in Figure 2 as a function of angle at fixed redshift ($z = 7$). The inclusion of galactic HI reduces the amplitude of the cross-correlation function by about 10% (relative to the case where galactic HI is ignored) late in the reionisation era for the reasons discussed in § 4.2. In addition, the cross-correlation changes sign at overlap because the HI content of the Universe shifts from being dominated by the underdense regions of IGM to HI in galaxies (which reside in overdense regions). This sign change will provide an unambiguous pointer to the redshift at which reionisation ends. Moreover, because the sign change will occur over a narrow frequency interval, it should provide an important check on possible sources of systematic error that could be present in measurements of the PS of intensity fluctuations which is always positive by construction.

6 MODEL-II: VARYING HOST MASS FOR GALACTIC HI

The calculations presented in Figures 1 and 2 assume that the galactic HI contributing to the 21-cm emission is found in the star forming systems. However it is possible that the connection between galactic HI and star formation is not direct, either because there is HI remaining in older low mass galaxies, or because the fraction of galactic gas that is HI is host mass dependent. As presented, our model is not able to address either of these issues. Therefore, to ascertain the possible range of influence that galactic HI might have on the 21-cm fluctuation statistics, we have assumed a characteristic mass M_{col} for the hosts of galactic HI, and replaced the expression for T_{IGM} (equation 14) with

$$T_{\text{IGM}}(\delta, R) = 22\text{mK} \left(\frac{1+z}{7.5} \right)^{1/2} \times \left[(1 - Q_{\delta,R}) \left(1 + \frac{4}{3}\delta \right) + x_{\text{HI,col}} \left(1 + \frac{4}{3}b\delta \right) \right], \quad (10)$$

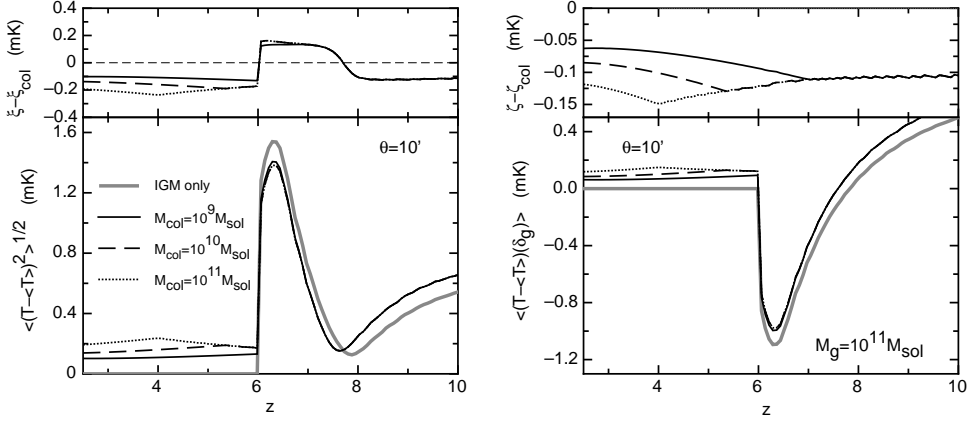


Figure 3. Model-II with fixed characteristic host mass for galactic HI. *Left:* The evolution of the auto-correlation function of brightness temperature with redshift (computed within regions of size $10'$). *Right:* The evolution of the cross-correlation function with redshift (computed within regions of size $10'$). In each case the grey and dark lines correspond to models which exclude and include galactic HI respectively. The small upper section of each panel shows the difference between the models without and including galactic HI.

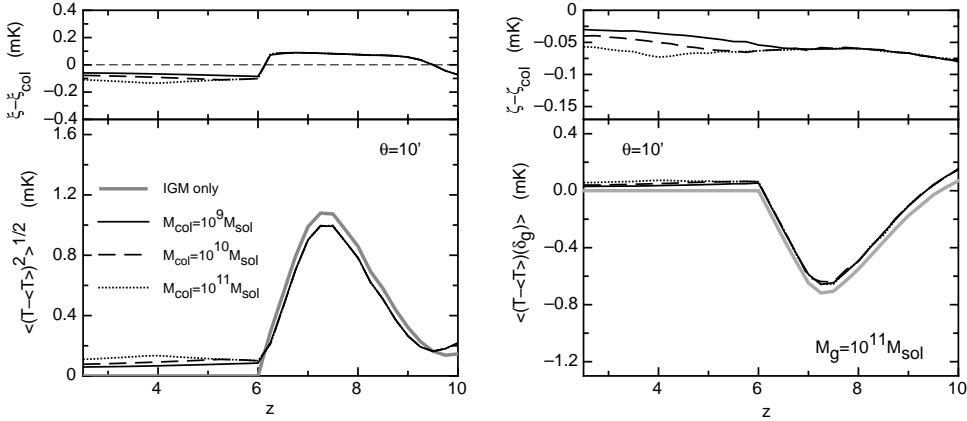


Figure 4. As per Figure 3, but computed using the semi-numeric rather than analytic model.

where we have defined the mass averaged fraction of cosmic hydrogen that is galactic HI ($x_{\text{HI,col}}$). We note that in order to maintain self consistency, the host mass of the galactic HI must correspond to a collapsed fraction $[F_{\text{col}}(M_{\text{col}})]$ that is in excess of $x_{\text{HI,col}}$. At a particular redshift the maximum possible host mass ($M_{\text{col},x}$) corresponding to a collapsed fraction that equals $x_{\text{HI,col}}$ is given by evaluation of

$$F_{\text{col}}(\delta, R, z, M_{\text{col},x}) = x_{\text{HI,col}}. \quad (11)$$

The host mass at which the galaxy bias (b) in equation (10) is evaluated is therefore

$$M = \min(M_{\text{col},x}, M_{\text{col}}). \quad (12)$$

With these modifications for the galactic HI distribution, we may compute the 21-cm fluctuation statistics as before using equation (7).

The resulting auto-correlation functions are shown in Figure 3 as a function of redshift at fixed angle ($\theta = 10'$). Three values for M_{col} are shown, $10^9 M_{\odot}$, $10^{10} M_{\odot}$ and $10^{11} M_{\odot}$. Late in the reionisation era, the amplitude of the auto-correlation function is decreased by $\sim 10\%$ (relative to the case where galactic HI is ignored). Below $z \sim 6$ larger,

more biased hosts of galactic HI result in a more significant increase of the fluctuation amplitude. However at $z \gtrsim 6$ $M_{\text{col},x} < M_c$, and hence our model predicts the same evolution for different values of M_{col} (see equation 12). The cross-correlation function is also shown in Figure 3. The cross-correlation changes sign at overlap as before. More massive hosts of the galactic HI result in a cross-correlation with a larger amplitude following reionisation.

7 SEMI-NUMERICAL SIMULATIONS

The analytic calculations described thus far provide a qualitative description of the effect of galactic HI on the statistics of 21-cm fluctuations and their association with galaxies. However, this analytic model is unable to describe fluctuations on scales comparable to the characteristic bubble scale once reionisation becomes established (Wyithe & Morales 2007). In the next section of this paper we therefore investigate the statistics of 21-cm fluctuations including galactic HI in a semi-numerical model for the reionisation of a three-dimensional volume of the IGM (Geil & Wyithe 2008;

Zahn et al. 2007; Mesinger & Furlanetto 2007). Our semi-numerical simulations are based on model-II with respect to the galactic HI contribution.

7.1 The ionisation field

Our modelling follows the procedure outlined in Geil & Wyithe (2008), and we refer the reader to that paper for details of the model. The model employs a semi-analytic prescription for the reionisation process, which is combined with a realisation of the density field. We construct an ionisation field based on a Gaussian random field for the overdensity of mass, combined with the value of the ionised fraction $Q_{\delta,R}$ (equation 1) as a function of overdensity δ and smoothing scale R . We repeatedly filter the linear density field at logarithmic intervals on scales comparable to the box size down to the grid scale size. For all filter scales, the ionisation state of each grid position is determined using $Q_{\delta,R}$ and deemed to be fully ionised if $Q_{\delta,R} \geq 1$. All voxels within a sphere of radius R centred on these positions are flagged and assigned $Q_{\delta,R} = 1$, while the remaining non-ionised voxels are assigned an ionised fraction of $Q_{\delta,R_{f,\min}}$, where $R_{f,\min}$ corresponds to the smallest smoothing scale. A voxel forms part of an HII region if $Q_{\delta,R} > 1$ on any scale R . In this paper we present simulations corresponding to a linear density field of resolution 256^3 , with a comoving side length of 512 Mpc. This procedure yields an ionisation map $Q_{\text{ion}}(\mathbf{x})$ as a function of position \mathbf{x} .

Having computed the ionisation field we then find the distribution of the galactic HI component. Rather than try to assign individual galaxies to the simulation we make the approximation that Poisson noise will be negligible and assign a smooth density of HI

$$\rho_{\text{HI,col}}(\vec{x}) = x_{\text{HI,col}} \rho_{\text{H}} [1 + b\delta(\vec{x})], \quad (13)$$

where $\rho_{\text{HI,col}}$ and ρ_{H} are the mass averaged densities of HI that is collapsed in galaxies, and the total hydrogen density respectively. The position dependent brightness temperature of the simulation box becomes

$$T_{\text{IGM}}(\vec{x}) = 22\text{mK} \left(\frac{1+z}{7.5} \right)^{1/2} \times [(1 - Q_{\text{ion}})(1 + \delta) + x_{\text{HI,col}}(1 + b\delta)]. \quad (14)$$

Note that our semi-numerical model does not compute peculiar velocities, and so equation (14) does not include a peculiar velocity induced enhancement of the brightness temperature in overdense regions. As in earlier sections we consider a model in which the mean IGM is reionised at $z = 6$. We again assume that star formation proceeds in halos above the hydrogen cooling threshold in neutral regions of IGM. In ionised regions of the IGM star formation is assumed to be suppressed by radiative feedback (see §2).

7.2 Variance in 21-cm emission

Since our semi-numerical model computes the three dimensional ionisation structure in the IGM, including the effect of HII regions, we can use it to compute the evolution of the variance. The resulting auto-correlation functions are shown in the left hand panel of Figure 4 as a function of redshift at fixed angle ($\theta = 10'$). As in the analytic model presented in

Figure 3, three values for M_{col} are shown, $10^9 M_{\odot}$, $10^{10} M_{\odot}$ and $10^{11} M_{\odot}$. These curves can be compared directly with the analytic approximation. This comparison shows that while the analytic model yields the correct qualitative behaviour, it is not quantitatively correct, both in terms of the redshift and amplitude of maximum fluctuations. However, in agreement with the analytic calculation, our semi-numerical calculations of the auto-correlation function show that the fluctuation amplitude is modified at the level of 10-20% (relative to the case where galactic HI is ignored) by the presence of a 2% galactic HI fraction throughout the reionisation era. The semi-numerical calculations of the cross-correlation function are also shown in the right hand panel of Figure 4 as a function of redshift at fixed angle ($\theta = 10'$). Comparison with Figure 3 also shows that the analytic calculation of the cross-correlation is qualitatively correct, but does not predict the correct quantitative evolution.

7.3 21-cm power spectrum

Figure 5 shows 21-cm PS computed from the semi-numerical simulations at $z = 7$ (left) and $z = 9$ (right). We plot the dimensionless PS $\Delta_{21}^2(k) = k^3/(2\pi^2)P_{21}(k)$, where P_{21} is the PS of 21-cm fluctuations. Both the case of the IGM alone (Δ_{21}^2), and the case assuming a host mass of $M_{\text{col}} = 10^{10} M_{\odot}$ for the galactic HI ($\Delta_{21,\text{col}}^2$) are shown (lower panels). We also show the relative fluctuation $\delta_{21,\text{col}} = (\Delta_{21}^2 - \Delta_{21,\text{col}}^2)/\Delta_{21}^2$ of the 21-cm PS owing to galactic HI (upper panels).

These figures illustrate the shoulder in the PS that corresponds to the typical bubble scale and which is due to the movement of power from small to large scales that accompanies the formation of HII regions. Because the galactic HI is biased towards HII regions, this movement of power is lessened when the contribution of galactic HI is considered. Hence the PS at large scales evaluated from simulations which include HI in galaxies is lower than the PS computed using the IGM alone. The effect of galactic HI is therefore to change the shape of the 21-cm PS rather than just the amplitude.

7.4 21cm-galaxy cross power spectrum

The central and upper panels of Figure 6 show the modulus of the dimensionless 21cm-galaxy cross PS with ($\Delta_{21,\text{g,col}}^2$) and without ($\Delta_{21,\text{g}}^2$) galactic HI as well as the galactic HI induced fluctuation [$\delta_{21,\text{g,col}} = (\Delta_{21,\text{g}}^2 - \Delta_{21,\text{g,col}}^2)/\Delta_{21,\text{g}}^2$], computed from the semi-numerical simulations at $z = 7$ (left) and $z = 9$ (right). Again a host mass of $M_{\text{col}} = 10^{10} M_{\odot}$ is considered for the galactic HI. An observed galaxy mass of $M_{\text{g}} = 10^{12} M_{\odot}$ is assumed. In the lower panels of Figure 6 we show the corresponding coefficient of the 21cm-galaxy cross PS.

Since overdense regions, where galaxies are concentrated, are reionised first these figures show an anti-correlation on large scales, which drops in strength to zero on small scales after the formation of HII regions. We find that the inclusion of galactic HI lessens the amplitude of the anti-correlation, since a fraction of HI is now co-located with the galaxies inside the HII regions. In addition, the cross PS

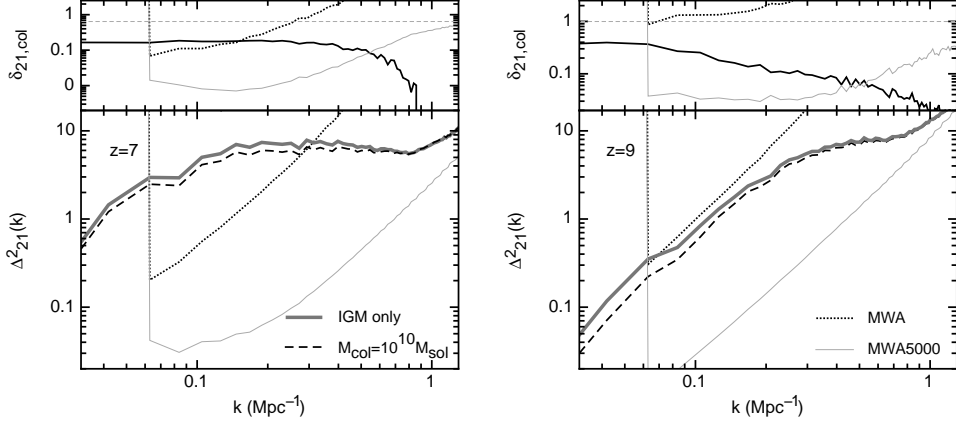


Figure 5. *Lower panels:* 21-cm power spectra computed using semi-numerical models at $z = 7$ (left) and $z = 9$ (right). In each case models are shown for a host mass of $M_{\text{col}} = 10^{10} M_{\odot}$ for the galactic HI, as well as for the IGM-only case. *Upper panels:* The relative perturbation on the PS due to galactic HI [$\delta_{21,\text{col}} = (\Delta_{21}^2 - \Delta_{21,\text{col}}^2)/\Delta_{21}^2$]. Also plotted for comparison is the estimated sensitivity (lower panels), and the sensitivity relative to Δ_{21}^2 (upper panels) within bins of width $\Delta k = k/10$ assuming 1000 hr integration on 1 field for the MWA and MWA5000 (dotted and thin-grey lines).

changes sign on small scales which reflects the correlation of galaxies with the galactic HI inside the H II regions, where no power is contributed in 21-cm fluctuations of the IGM. Thus, with the caveat that galaxies can be selected without bias from IGM absorption (which may not be true if, for instance, the galaxies are selected in Ly α emission—see Lidz et al 2008 for discussion for the latter case), the scale at which the 21-cm-galaxy cross PS changes sign could be used to probe the scale of H II regions late in the reionisation era.

8 SENSITIVITY TO THE EFFECT OF GALACTIC HI ON 21-CM FLUCTUATIONS

Before concluding, we compute the sensitivity with which the effect of galactic HI could be detected using forthcoming low-frequency arrays.

8.1 Sensitivity to the 21-cm PS

To compute the sensitivity $\Delta P_{21}(\vec{k})$ of a radio-interferometer to the 21-cm PS, we follow the procedure outlined by McQuinn et al. (2006) and Bowman, Morales & Hewitt (2007) [see also Wyithe, Loeb & Geil (2008)]. The important issues are discussed below, but the reader is referred to these papers for further details. The sensitivity to the PS comprises components due to the thermal noise, and due to sample variance within the finite volume of the observations. We consider observational parameters corresponding to the design specifications of the MWA, and of a hypothetical followup to the MWA (termed the MWA5000). In particular the MWA is assumed to comprise a phased array of 500 tiles. Each tile contains 16 cross-dipoles to yield an effective collecting area of $A_e = 16(\lambda^2/4)$ (the area is capped for $\lambda > 2.1\text{m}$). The physical area of a tile is $A_{\text{tile}} = 16\text{m}^2$. The tiles are distributed according to a radial antenna density of $\rho(r) \propto r^{-2}$, within a diameter of 1.5km and outside of a flat density core of radius 18m. The MWA5000 is assumed to follow the basic design of the MWA. The quantitative

differences are that the telescope is assumed to have 5000 tiles within a diameter of 2km, with a flat density core of 80m. In each case we assume 1 field is observed for 1000 hr. Following the work of McQuinn et al. (2006) we assume that foregrounds can be removed over 8MHz bins, within a bandpass of 32MHz [foreground removal therefore imposes a minimum on the wave-number accessible of $k_{\text{min}} \sim 0.04[(1+z)/7.5]^{-1}\text{Mpc}^{-1}$].

The sensitivity to the 21-cm PS per mode may be written

$$\delta P_{21}(k, \theta) = \left[\frac{T_{\text{sky}}^2}{\Delta \nu_{\text{int}}} \frac{D^2 \Delta D}{n(k_{\perp})} \left(\frac{\lambda^2}{A_e} \right)^2 \right] + P_{21}(k, \theta), \quad (15)$$

where D is the co-moving distance to the centre of the survey volume which has a co-moving depth ΔD . Here $n(k_{\perp})$ is the density of baselines which observe a wave vector with transverse component k_{\perp} , and θ is the angle between the mode \vec{k} and the line of sight. The thermal noise component (first term) is proportional to the sky temperature, where $T_{\text{sky}} \sim 250 \left(\frac{1+z}{7} \right)^{2.6} \text{K}$ at the frequencies of interest. The second term corresponds to sample variance. The overall sensitivity is

$$\Delta P_{21}(k, \theta) = \delta P_{21}(k, \theta) / \sqrt{N_c(k, \theta)}, \quad (16)$$

where $N_c(k, \theta)$ denotes the number of modes observed in a k -space volume $d^3 k$ (only modes whose line-of-sight components fit within the observed band-pass are included). In terms of the k -vector components k and θ , $N_c = 2\pi k^2 \sin \theta dk d\theta \mathcal{V} / (2\pi)^3$ where $\mathcal{V} = D^2 \Delta D (\lambda^2 / A_e)$ is the observed volume. Taking the spherical average over bins of θ , the sensitivity to the 21-cm PS is

$$\frac{1}{[\Delta P_{21}(k)]^2} = \sum_{\theta} \frac{1}{[\Delta P_{21}(k, \theta)]^2}. \quad (17)$$

The spherically averaged sensitivity curves for the MWA (within bins of $\Delta k = k/10$) are plotted as the dotted lines in the lower panels of Figure 5. The sensitivity as a ratio of the PS computed without a galactic HI contribution ($\Delta P_{21}/P_{21}$) is plotted in the upper panels of Figure 5

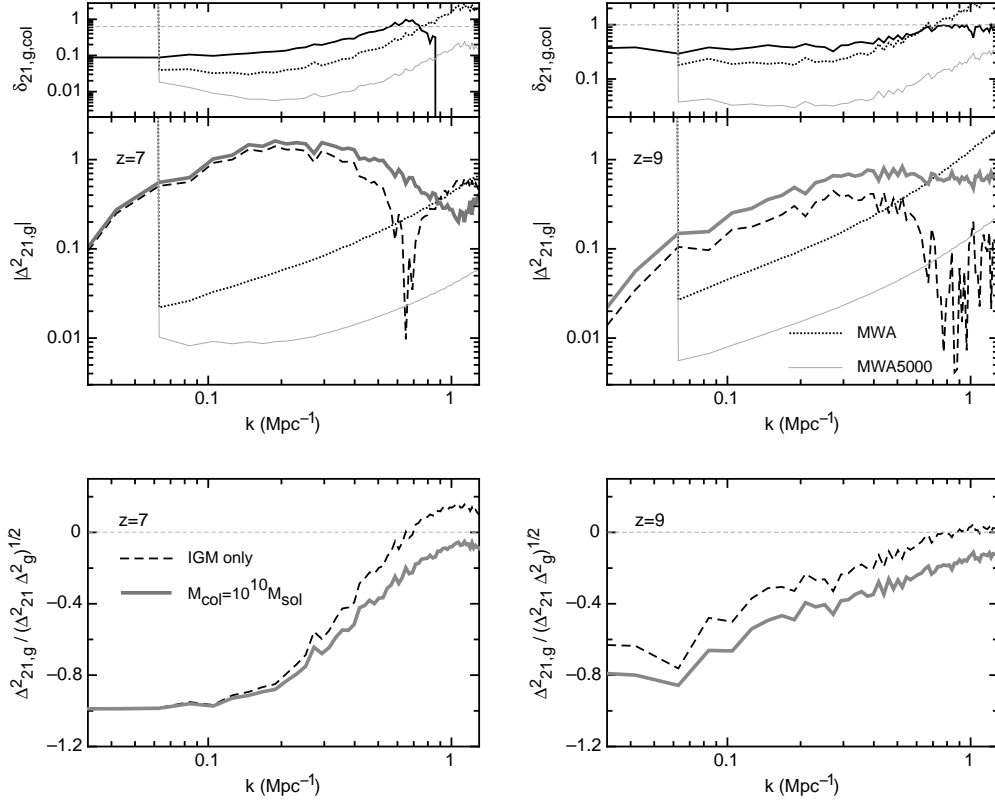


Figure 6. 21cm-galaxy cross PS computed using semi-numerical models. *Central and Lower panels:* The modulus and coefficient of the 21cm-galaxy cross PS respectively computed at $z = 7$ (left) and $z = 9$ (right). In each case models are shown assuming a host mass of $M_{\text{col}} = 10^{10} M_{\odot}$ for the galactic HI, as well as the IGM-only case. The host mass of observed galaxies is assumed to be $M_g = 10^{11} M_{\odot}$. *Upper panels:* The relative perturbation on the PS due to galactic HI [$\delta_{21,g,col} = (\Delta_{21,g}^2 - \Delta_{21,g,col}^2) / \Delta_{21,g}^2$]. Also plotted for comparison is the estimated sensitivity (central panels), and the sensitivity relative to $\Delta_{21,g}^2$ (upper panels) within bins of width $\Delta k = k/10$ assuming 1000 hr integration on 1 field for the MWA and MWA5000 (dotted and thin-grey lines). To estimate this sensitivity galaxies were assumed to be observed down to $M_g = 10^{11} M_{\odot}$ over the entire field.

(again as dotted lines). These estimates illustrate that late in reionisation, the effect of the galactic HI will be at a level above the sensitivity of the first generation low-frequency arrays. However, the low resolution of the MWA would mean that the shape-change of the PS owing to the galactic HI would not be detected until very close to overlap. The corresponding sensitivity curves for the MWA5000 are plotted as the thin grey lines in Figure 5. The larger collecting area of the MWA5000 would allow the effect of galactic HI to be detected out to higher redshifts and at smaller scales.

8.2 Sensitivity to the 21cm-galaxy cross PS

To compute the sensitivity of the MWA to the 21cm-galaxy cross PS ($P_{21,g}$) we follow the discussion of Furlanetto & Lidz (2007). The sensitivity to a particular mode is

$$2[\delta P_{21,g}(k, \theta)]^2 = [P_{21,g}(k, \theta)]^2 + \delta P_{21}(k, \theta) \delta P_g(k, \theta), \quad (18)$$

where $\delta P_g(k, \theta) = b^2 P_{\delta}(k, \theta) + n_g^{-1}$ is the uncertainty in the galaxy PS, and P_{δ} is the underlying mass PS⁶ at redshift

⁶ Note that for consistency with our estimate of the 21-cm PS, we are neglecting redshift space distortions in calculation of the galaxy PS.

z . In the second term n_g is the density of galaxies (which we approximate as $n_g = M_g dn/dM_g$, where dn/dM_g is the Press-Schechter 1976) mass function and M_g is the halo mass of galaxies in the survey⁷. After calculation of the total sensitivity

$$\Delta P_{21,g}(k, \theta) = \delta P_{21,g}(k, \theta) / \sqrt{N_c(k, \theta)}, \quad (19)$$

and taking the spherical average over bins of θ as before, the sensitivity to the 21cm-galaxy cross PS is

$$\frac{1}{[\Delta P_{21,g}(k)]^2} = \sum_{\theta} \frac{1}{[\Delta P_{21,g}(k, \theta)]^2}. \quad (20)$$

The spherically averaged sensitivity curves for the MWA (within bins of $\Delta k = k/10$) are plotted as the dotted lines in the central panels of Figure 6. The sensitivity as a ratio of the fiducial IGM only PS ($\Delta P_{21,g}/P_{21,g}$) is also plotted in the upper panels of Figure 6. Here we have assumed that galaxies have been detected down to a resolution limit corresponding to a host mass of $M_g = 10^{11} M_{\odot}$ over the full MWA field. These sensitivity estimates illustrate that the effect of the galactic HI on the cross-correlation between

⁷ Note that we have neglected redshift errors when computing the Poisson component of the uncertainty in the galaxy PS.

galaxies and 21-cm emission could be detected with the first generation low-frequency arrays. Moreover the resolution of the MWA would be sufficient to detect the sign-change of the 21cm-galaxy cross PS at the scale of the H II regions late in reionisation. The corresponding sensitivity curves for the MWA5000 are plotted as the thin grey lines in Figure 6. The larger collecting area of the MWA5000 would greatly increase the significance with which the effect of galactic H I could be measured.

9 CONCLUSION

In this paper we have investigated the impact of H I in galaxies on the statistics of 21-cm fluctuations using analytic and semi-numerical models. Our models are unable to self-consistently compute the galactic H I content of galaxies prior to the end of reionisation. As an input to our model we have therefore assumed that during the reionisation era 2% of hydrogen is in the form of H I and located within galaxies. This number is motivated by observations of the mass weighted fraction of cosmic hydrogen in H I after the end of reionisation, which is dominated by damped absorption systems and which has a constant value of $\sim 2\%$ between $z \sim 1$ and $z \sim 5$. Our modelling shows that this assumption results in a reduction of 10-20% in the amplitude of 21-cm fluctuations over a range of spatial scales, and over a large fraction of the reionisation era. In addition to the amplitude of 21-cm fluctuations we have also modelled the cross-correlation between galaxies and 21-cm emission. We find that the inclusion of galaxies decreases the amplitude of the cross-correlation by a few tens of percent. In addition, the cross-correlation between galaxies and 21-cm emission will change sign at the end of the reionisation era, providing an alternative avenue to pinpoint the end of reionisation.

We find that our analytic estimates become less applicable once H II regions become a dominant feature of the IGM. We have therefore supplemented our analytic estimates with semi-numerical modelling of the three dimensional ionisation structure of the IGM. We find that the qualitative conclusions from our analytic calculations are vindicated by this modelling. In addition to the above estimates of auto and cross-correlation, we have used our semi-numerical model to compute 21-cm power spectra, and 21cm-galaxy cross power spectra. The effect of galactic H I is to change the shape of the 21-cm PS rather than just the amplitude. In particular, because the galactic H I is biased towards H II regions, we find that the H II region induced *shoulder* in the PS is less prominent when the contribution of galactic H I is considered.

The amplitude of the 21-cm PS is modified in a scale dependent way by up to 20% when a 2% galactic H I fraction is included. Of course the galactic H I fraction is very uncertain at high redshift. However we find that the fractional modification of the 21-cm fluctuation statistics is approximately proportional to the density of galactic H I. Therefore, if we assume a value lower (higher) than the 2% observed at $z < 5$, then our results for the error introduced through neglect of galactic H I will be over (under)estimated. On the other hand, the change of sign in the cross-correlation between galaxies and the 21-cm signal is robust to our assumptions.

We find that the inclusion of galactic H I lessens the

amplitude of the anti-correlation between galaxies and 21-cm emission since a fraction of H I is now co-located with the galaxies inside the H II regions. In addition, the cross PS changes sign on small scales, which reflects the correlation of galaxies with the galactic H I inside the H II regions, where no power is contributed in 21-cm fluctuations of the IGM. Thus, the scale at which the 21cm-galaxy cross PS changes sign could be used to probe the scale of H II regions late in the reionisation era.

We have estimated the sensitivity of the MWA to the spherically averaged 21-cm PS and 21cm-galaxy cross PS. Our calculations illustrate that the effect of the galactic H I on 21-cm fluctuations is at a level that would be significant with respect to the sensitivity of the MWA late in reionisation. However the low resolution of the MWA would mean that the shape change of the PS owing to the galactic H I could not be detected until very close to overlap. On the other hand, when combined with a suitable galaxy redshift survey, the resolution of the MWA would be sufficient to detect the sign change of the 21cm-galaxy cross PS at the scale of the H II regions late in reionisation. A followup telescope comprising 10 times the collecting area of the MWA would measure the effects of galactic H I with high significance.

In summary, our modelling shows that the H I content of the galaxies that reionise the universe provides a significant contribution to the statistics of 21-cm fluctuations. The galactic H I contribution to the 21-cm intensity will therefore need to be considered in detailed modelling of the 21-cm intensity PS in order to correctly interpret measurements from the next generation of low-frequency arrays.

Acknowledgements The research was supported by the Australian Research Council (JSBW). LW and PMG acknowledge the support of Australian Postgraduate Awards. SPO acknowledges support from NASA grant NNG06GH95G.

REFERENCES

- Barkana, R., & Loeb, A. 2005, *ApJL*, 624, L65
- Barkana, R. 2007, *MNRAS*, 376, 1784
- Bharadwaj, S., & Ali, S. S. 2005, *MNRAS*, 356, 1519
- Bond, J. R., Cole, S., Efstathiou, G., & Kaiser, N. 1991, *ApJ*, 379, 440
- Bowman, J., Morales, M., Hewitt, J., 2005, *ApJ*, 638, 20
- Bowman, J. D., Morales, M. F., & Hewitt, J. N. 2007, *ApJ*, 661, 1
- Dijkstra, M., Haiman, Z., Rees, M. J., & Weinberg, D. H., *Astrophys. J.*, 601, 666-675 (2004)
- Efstathiou, G., *Mon. Not. R. Astron. Soc.*, 256, 43-47 (1992)
- Fan, X., et al. 2006, *AJ*, 132, 117
- Furlanetto, S. R., Zaldarriaga, M., & Hernquist, L. 2004, *ApJ*, 613, 16
- Furlanetto, S. R., Oh, S. P., & Briggs, F. H. 2006, *Physics Reports*, 433, 181
- Furlanetto, S. R., & Lidz, A. 2007, *ApJ*, 660, 1030
- Geil, P. M., & Wyithe, J. S. B. 2008, *MNRAS*, 386, 1683
- Gnedin, N. Y., & Fan, X. 2006, *ApJ*, 648, 1
- Iliev, I. T., Mellema, G., Pen, U.-L., Bond, J. R., & Shapiro, P. R. 2008, *MNRAS*, 384, 863
- Kashikawa, N., et al. 2006, *ApJ*, 648, 7

- Komatsu, E., et al. 2008, ArXiv e-prints, 803, arXiv:0803.0547
- Kramer, R. H., Haiman, Z., & Oh, S. P. 2006, ApJ, 649, 570
- Lidz, A., Zahn, O., Furlanetto, S., McQuinn, M., Hernquist, L., & Zaldarriaga, M. 2008, ArXiv e-prints, 806, arXiv:0806.1055
- McQuinn, M., Zahn, O., Zaldarriaga, M., Hernquist, L., & Furlanetto, S. R. 2006, ApJ, 653, 815
- Mesinger, A., & Furlanetto, S. 2007, ApJ, 669, 663
- Mo, H. J., & White, S. D. M. 1996, MNRAS, 282, 347
- Morales, M. F., Bowman, J. D., & Hewitt, J. N. 2006, ApJ, 648, 767
- Press, W., Schechter, P., 1974, ApJ., 187, 425
- Prochaska, J. X., Herbert-Fort, S., & Wolfe, A. M. 2005, ApJ, 635, 123
- Quinn, T., Katz, N., & Efstathiou, G., 278, L49-L54 (1996)
- Shapiro, P. R., Iliev, I. T., & Raga, A. C. 2004, MNRAS, 348, 753
- Thoul, A. A., & Weinberg, D. H., Astrophys. J., 465, 608-116 (1996)
- White, R., Becker, R., Fan, X., Strauss, M., 2003, Astron J., 126, 1
- Wyithe, J. S. B., & Loeb, A. 2007, MNRAS, 375, 1034
- Wyithe, J. S. B., Loeb, A., & Geil, P. M. 2008, MNRAS, 383, 1195
- Wyithe, J. S. B., & Morales, M. F. 2007, MNRAS, 379, 1647
- Zahn, O., Lidz, A., McQuinn, M., Dutta, S., Hernquist, L., Zaldarriaga, M., & Furlanetto, S. R. 2007, ApJ, 654, 12
- Zaldarriaga, M., Furlanetto, S. R., & Hernquist, L. 2004, ApJ, 608, 622